

The Pennsylvania State University

The Graduate School

A U-Pb CA-ID-TIMS date ($230.964 \text{ Ma} \pm 0.077 \text{ Ma}$) for the Maple
Creek Gabbro, Wrangellia Large Igneous Province, Kluane Range,
the Yukon

A Thesis in

Geosciences

by

Kathleen Grosswiler

© 2022 Kathleen Grosswiler

Submitted in Partial Fulfillment

of the Requirements

for the Degree of

Master of Science

December 2022

The thesis of Kate Grosswiler was reviewed and approved by the following:

Brian Kelley
Assistant Professor of Geosciences
Thesis Advisor

Mark Patzkowsky
Professor of Geosciences

Jesse Reimink
Assistant Professor of Geosciences

Donald Fisher
Professor of Geosciences
Associate Head of the Graduate Programs and Research

ABSTRACT

The eruption of the Wrangellia Large Igneous Province (LIP) has long been implicated in Carnian (early Late Triassic) biotic revolution and Earth-system change, but its timing is poorly constrained. Published U-Pb, Ar-Ar, and K-Ar radioisotopic dates for the Wrangellia LIP have a broad range of uncertainties (0.53 to 13.5 Myr), making them too imprecise to definitively establish the link between the environmental changes that occurred during the Carnian and Wrangellia volcanism. The Wrangellia LIP is found in Alaska, the Yukon, and British Columbia. Improvements in analytical methods, such as using chemical abrasion in IDTIMS zircon geochronology, have reduced uncertainties, allowing us to place more precise geochronologic constraints on the timing of Wrangellia magmatism. In this study, I used high-precision U-Pb chemical abrasion isotope dilution thermal ionization mass spectrometry (CA-IDTIMS) to date a Maple Creek gabbro from the Tatamagouche Creek area of Yukon to investigate the timing of Wrangellia volcanism and assess its temporal connection to Carnian Earth system change. The Maple Creek gabbro is interpreted to be a feeder for the extrusive Wrangellia Nikolai flood basalts. The analysis produced a date of 230.964 ± 0.077 Ma. This date is currently the most precise radioisotopic constraint for Wrangellia volcanism. The date also overlaps within uncertainty with a U-Pb age of 230.91 ± 0.33 Ma from a volcanic ash in the Apennines mountains in southern Italy that stratigraphically overlies sedimentary evidence for Carnian environmental perturbations. In combination, these dates provide the best evidence of the temporal coincidence between Wrangellia volcanism and Carnian Earth system change.

TABLE OF CONTENTS

List of tables.....	v
List of Figures.....	v
Acknowledgements.....	viii
Introduction.....	1
Geologic Setting.....	4
Methods.....	8
Results.....	13
Discussion.....	17
Summary and Conclusion.....	21
References.....	23

LIST OF FIGURES

- Figure 1: The extent of the Wrangellia Large Igneous Province, now exposed in parts of Alaska, the Yukon, and British Columbia. Modified from Greene et al., (2010)..... 2
- Figure 2: Published radioisotopic dates for the Wrangellia LIP and their corresponding uncertainties. The dates are separated by dating method (color) and location (shape) (Schmidt and Rogers, 2007; Greene et al., 2010; Bittenbender et al., 2003; Bittenbender et al., 2007; Lassiter, 1995, Mortensen and Hulbert, 1992, Campbell, 1981; Sluggett, 2003. Parrish and McNicoll, 1992). The grey band denotes the approximate timing and duration of the CPE..... 3
- Figure 3: Late-Triassic paleogeographic reconstruction. The paleogeographic location of the Wrangellia LIP is shown. Modified from image created by Kieff, distributed under the Creative Commons Attribution-Share Alike 3.0 Unported license. 5
- Figure 4: Approximate locations of the samples from this study. The location of the Maple Creek gabbro sample that yielded zircons is shown in green. The samples shown in red were processed but did not yield zircons. This figure was created using ArcGIS.. 6
- Figure 5: Simplified stratigraphic column for the Tatamagouche Creek area. Modified from Mortensen and Hulbert (1992). The approximate stratigraphic location of the dated sample is indicated by the green star. 7
- Figure 6: Zircons extracted using the whole rock dissolution method before (left) and after (right) chemical abrasion at 190° C for 12 hours. 12 of the 12 grains that were chemically abraded survived the process..... 11
- Figure 7: Zircons extracted using traditional methods before (left) and after (right) chemical abrasion at 190 ° C for 12 hours. Only 3 of the 12 grains that were chemically abraded survived the process. None of them were suitable for IDTIMS analysis. This indicates that the whole rock dissolution process eliminated the most metamict and damaged zircons, streamlining the selection process for TIMS analysis. 12
- Figure 8: Hand sample and zircons from the dated sample 04-SIS-165-1; a sample of the Maple Creek gabbro collected in the Tatamagouche area of the Kluane Range, Yukon. The zircons pictured on the right were collected using the whole rock dissolution method..... 14

- Figure 9:** Weighted mean results for sample 04-SIS-165-1. Of the six grains analyzed, two were excluded from the final date calculations. The four concordant zircons from sample 04-SIS-165-1 were used to calculate the mean weighted date and yielded a result of 230.964 with a 2 sigma (find symbol) uncertainty of +/- 0.077 Ma..... 15
- Figure 10:** Concordia diagram for sample 04-SIS-165-1. Of the six grains analyzed, two were excluded from the final date calculations. The excluded analyses are shown in light grey, and the analyses used are shown in blue. The oldest analysis was not included because the result was reversely discordant, which may indicate that there was xenocrystic inheritance in that grain. The youngest date was also not included, as the slightly younger date is interpreted to be a result of minor lead loss..... 16
- Figure 11:** Published radioisotopic dates for the Wrangellia LIP and their corresponding uncertainties, including the date from this study. The dates are separated by method (color) and location (shape) (Schmidt and Rogers, 2007; Greene et al., 2010; Bittenbender et al., 2003; Bittenbender et al., 2007; Lassiter, 1995; Mortensen and Hulbert, 1992; Campbell, 1981; Sluggett, 2003. Parrish and McNicoll, 1992). The grey band denotes the approximate timing and duration of the CPE. 18

LIST OF TABLES

<p>Table 1: List of samples received from the Yukon Geological Survey as potential candidates for the whole rock dissolution process. Of these samples, only one yielded zircons. The amygdaloidal basalt samples showed significant alteration and were excluded from consideration.</p>	9
<p>Table 2: Isotopic data for zircons from Maple Creek Gabbro. (a) z1, z2, etc. are labels for single zircon grains or fragments annealed and chemically abraded after Mattinson (2005); bold indicates grains used in final age calculations. (b) Model Th/U ratio iteratively calculated from the radiogenic $^{208}\text{Pb}/^{206}\text{Pb}$ ratio and $^{206}\text{Pb}/^{238}\text{U}$ age. (c) Pb* and Pbc represent radiogenic and common Pb, respectively; mol % $^{206}\text{Pb}^*$ with respect to radiogenic, blank, and initial common Pb. (d) Measured ratio corrected for spike and fractionation only. Pb fractionation corrected using mass bias measured in ET2535-spiked samples run during the experiment; U fractionation corrected based upon the measured ET535 spike composition during the run. € Corrected for fractionation, spike, and common Pb; all common Pb was assumed to be procedural blank: $^{206}\text{Pb}/^{204}\text{Pb} = 18.042 \pm 0.61\%$; $^{207}\text{Pb}/^{204}\text{Pb} = 15.537 \pm 0.52\%$; $^{208}\text{Pb}/^{204}\text{Pb} = 37.686 \pm 0.63\%$ (all uncertainties 1-sigma). (f) Errors are 2-sigma, propagated using the algorithms of Schmitz and Schoene (2007). (g) Calculations are based on the decay constants of Jaffey et al. (1971). $^{206}\text{Pb}/^{238}\text{U}$ and $^{207}\text{Pb}/^{206}\text{Pb}$ ages corrected for initial disequilibrium in $^{230}\text{Th}/^{238}\text{U}$ using $\text{Th}/\text{U} [\text{D}] = 0.2 \pm 0.05$.....</p>	14

ACKNOWLEDGEMENTS

I would like to thank my advisor, Dr. Brian Kelley, and all of the students that work in the Kelley lab. I would like to thank Steve Israel and Maurice Colpron from the Yukon Geological Survey for sending me the samples that I processed for my research. I would also like to thank Jim Crowley and Mark Schmitz for letting me do my laboratory work at Boise State University's Isotope Geology Laboratory, and for providing fantastic mentorship. I would like to also thank my partner Christopher Reynolds, my lab mate Garrett, my friend Thomas Farrell, and my wonderful family.

Introduction:

Large igneous provinces (LIPs) and associated volatile release are recognized as fundamental drivers of Earth system and biotic change (Bond and Sun, 2021; Wignall, 2001), but the temporal relationship between these processes is often poorly constrained. LIP volcanism affects atmospheric composition primarily through the release of CO₂ and other volatiles, potentially leading to global climate change and mass extinction (Bond and Sun, 2021; Wignall 2001). To better constrain the relationship between LIP volcanism, Earth system change, and biotic evolution, it is critical to accurately establish the timing of individual LIPs relative to intervals of Earth system change recorded in the sedimentary and fossil records (Burgess et al., 2015; Schoene et al., 2018). One of the most important and understudied LIPs is the Triassic Wrangellia Large Igneous Province, now exposed in parts of Alaska, the Yukon, and Vancouver Island, British Columbia (Fig. 1) (Greene et al., 2010). The initiation of the Wrangellia large igneous province has long been suggested as a potential causal mechanism for substantial environmental changes during the Carnian stage of the Late Triassic. This interval is commonly known as the Carnian Pluvial Episode (CPE) (Bond and Sun, 2021; Lu et al., 2021; Dal Corso et al., 2020). Although Wrangellia is often linked to the CPE, the temporal connection is tenuous because the radioisotopic dates for the Wrangellia LIP have large uncertainty ranges (Greene et al., 2010) and lack the precision necessary to definitively link it to Carnian Earth system change (Dal Corso et al., 2020).



Figure 1: The extent of the Wrangellia Large Igneous Province, now exposed in parts of Alaska, the Yukon, and British Columbia. Modified from Greene et al., (2010).

Published radioisotopic dates for Wrangellia magmatism span from 224 Ma \pm 8 Ma to 232.8 \pm 11.5 Ma and have broad uncertainties ranging from 0.5 to 13.2 Myr (Fig. 2) (Greene et al., 2010). These dates were obtained using potassium-argon (K–Ar), argon-argon (Ar–Ar), lead-lead (Pb–Pb) and uranium-lead (U–Pb) geochronology (Fig. 2). The dating techniques used are problematic in different ways. A substantial amount of Wrangellia basalts are altered, which impacts the reliability of the K–Ar and Ar–Ar dates (Greene et al., 2010). The published U–Pb dates were done before chemical abrasion was developed (Parish and McNicoll, 1992; Sluggett, 2003). Chemical abrasion was designed to help eliminate damaged zones of zircon crystals, making the results more accurate (Mattinson, 2005).

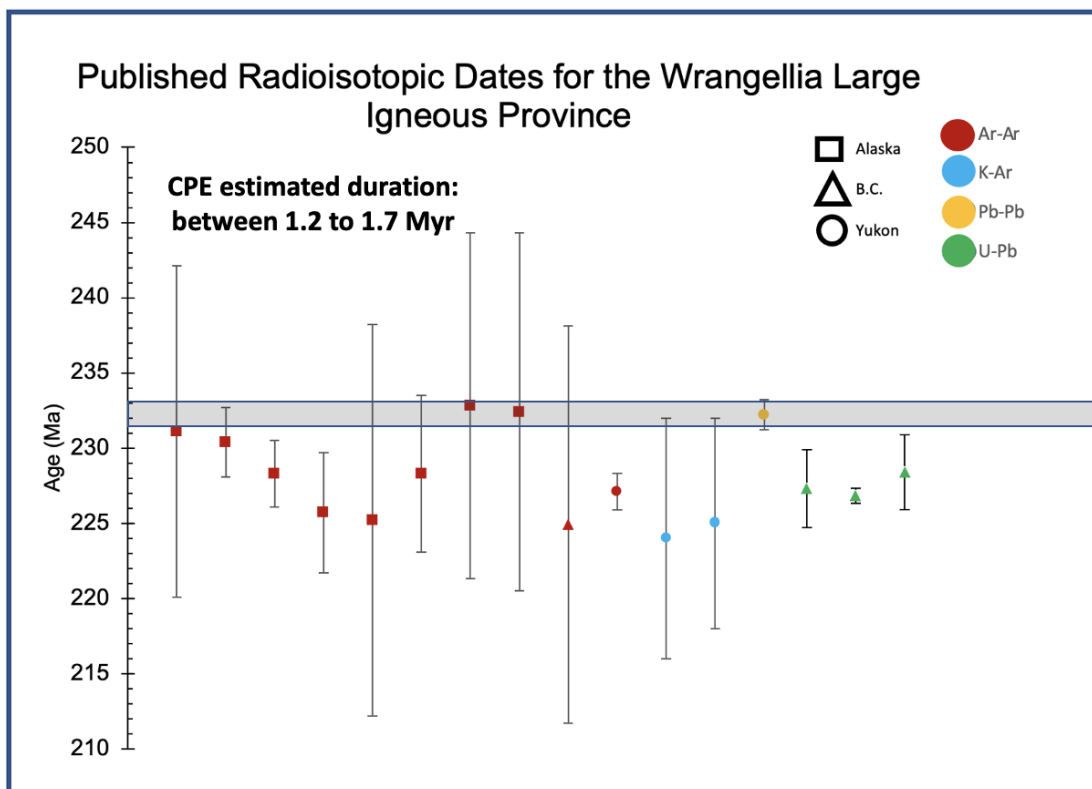


Figure 2: Published radioisotopic dates for the Wrangellia LIP and their corresponding uncertainties. The dates are separated by dating method (color) and location (shape) (Schmidt and Rogers, 2007; Greene et al., 2010; Bittenbender et al., 2003; Bittenbender et al., 2007; Lassiter, 1995; Mortensen and Hulbert, 1992; Campbell, 1981; Sluggett, 2003; Parrish and McNicoll, 1992). The grey band denotes the approximate timing and duration of the CPE.

During the CPE, environmental changes such as temperature increase of up to 7°C (Sun et al., 2018) and increased hydrologic cycling (Lu et al., 2021) led to extinction and substantial reorganization of marine and terrestrial ecosystems (Dal Corso et al., 2020). An estimated 33% of marine genera went extinct, making it one of the more consequential extinction events during the Mesozoic (Dal Corso et al., 2020). Although the extinction was less severe than the five major mass extinction events (Guex et al., 2016), it still had a profound impact on marine and terrestrial ecosystems (Dal Corso et al., 2020). In the aftermath of the extinction, dinosaurs radiated (Bernardi et al., 2018), scleractinian corals

started building reefs that resemble their modern counterparts (Martindale et al., 2019), and calcareous nanoplankton emerged (Furin et al., 2006; Erba, 2006). The CPE is estimated to have lasted approximately 1.2 to 1.7 million years, based on magnetostratigraphic, biostratigraphic and cyclostratigraphic constraints (Miller et al., 2017; Bernardi et al., 2018; Dal Corso et al., 2020).

In this study, I used chemical abrasion isotope dilution thermal ionization mass spectrometry (CA-IDTIMS) zircon geochronology on gabbro and ultramafic samples collected in the Kluane range, Yukon to investigate the timing of Wrangellia volcanism. CA-IDTIMS zircon geochronology offers unparalleled precision and accuracy (Schmitz et al., 2020), providing an opportunity to establish the best constraints for the timing of Wrangellia volcanism and to determine its temporal connection with the CPE.

Geologic setting:

The Wrangellia LIP formed as a massive oceanic plateau during the Middle to Late Triassic and accreted to western Pangea in the Late Jurassic or Early Cretaceous (Fig. 3) (Csejtey et al., 1982). Wrangellia is comprised of subaerial and subaqueous flood basalts and their associated intrusive units that acted as feeder networks for the flood basalts (Lassiter, 1995). The flood basalts are subdivided into two units, based on location: the Nikolai formation, found in Alaska and the Yukon, and the Karmutsen formation, found on Queen Charlotte Island and Vancouver Island, BC (Jones et al., 1977). Though they are subdivided based on geographic location, the units are inferred to be contemporaneous (Greene et al., 2010).

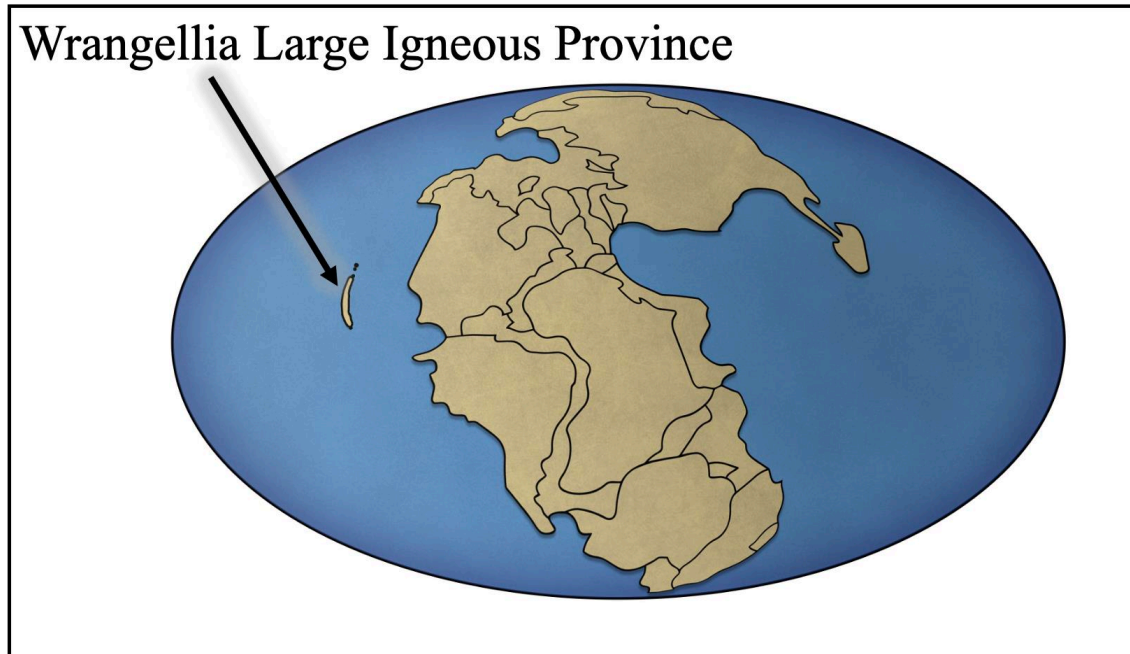


Figure 3: Late-Triassic paleogeographic reconstruction. The paleogeographic location of the Wrangellia LIP is shown. Modified from image created by Kieff, distributed under the Creative Commons Attribution-Share Alike 3.0 Unported license.

Wrangellia may have the most extensive exposures of any obducted oceanic plateau on earth, with between 93,000 km³ and 140,000 km³ of accreted material (Greene et al., 2010). Complete sections of the volcanic stratigraphy where the top and the base are preserved are found in locations on Vancouver Island and in Alaska (Richards et al., 1991). However, portions of Wrangellia were subducted underneath the western margins of North America, and its original volume remains unknown (Lassiter, 1995). There are several published estimates for the minimum original volume of Wrangellia, ranging from 140,000 km³ for the Karmutsen flood basalts (Greene et al., 2010) to 340,000 km³ for the Karmutsen flood basalts and the Nikolai flood basalts located in Alaska (Carlisle and Suzuki, 1974), to 1,000,000 km³ for the entire Wrangellia LIP (Lassiter, 1995 via Panuska, 1990). Each of the published volumes were calculated using estimated accumulation rates, estimated

stratigraphic thickness, and estimated duration of emplacement (Carlisle and Suzuki, 1974; Lassiter, 1995 via Panuska, 1990; Greene et al., 2010). However, the accumulation rate and estimated duration was different for each of the published volumetric estimates, causing the estimates to be substantially different from one another (Carlisle and Suzuki, 1974; Lassiter, 1995 via Panuska, 1990; Greene et al., 2010).

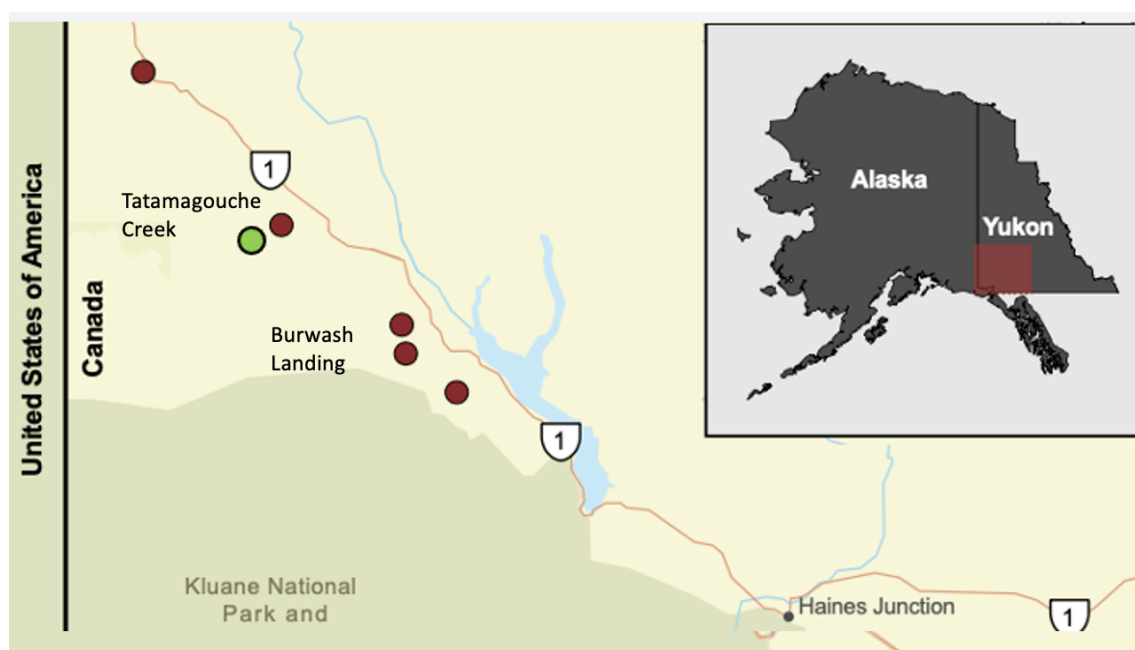


Figure 4: Approximate locations of the samples from this study. The location of the Maple Creek gabbro sample that yielded zircons is shown in green. The samples shown in red were processed but did not yield zircons. This figure was created using ArcGIS.

Wrangellia basalts in the Yukon are the most extensive in the Kluane Range, where approximately 1000 meters of strata are exposed (Israel et al., 2005). The mafic and ultramafic feeder sills for the overlying Nikolai flood basalts in the Yukon intrude into Paleozoic sedimentary formations (Hulbert, 1997). Samples for this study were collected in the Tatamagouche Creek and Burwash landing areas of the Kluane Range (Fig. 4). The Tatamagouche Creek area is home to the Tatamagouche Creek Intrusive Complex, which

includes the Kluane ultramafic suite and the Maple Creek gabbro (Fig. 5) (Mortensen and Hulbert, 1992; Hulbert, 1997). The Maple Creek gabbro and the Kluane ultramafic suite are interpreted to be the feeder system for the Nikolai flood basalts (Mortensen and Hulbert, 1992; Hulbert, 1997).

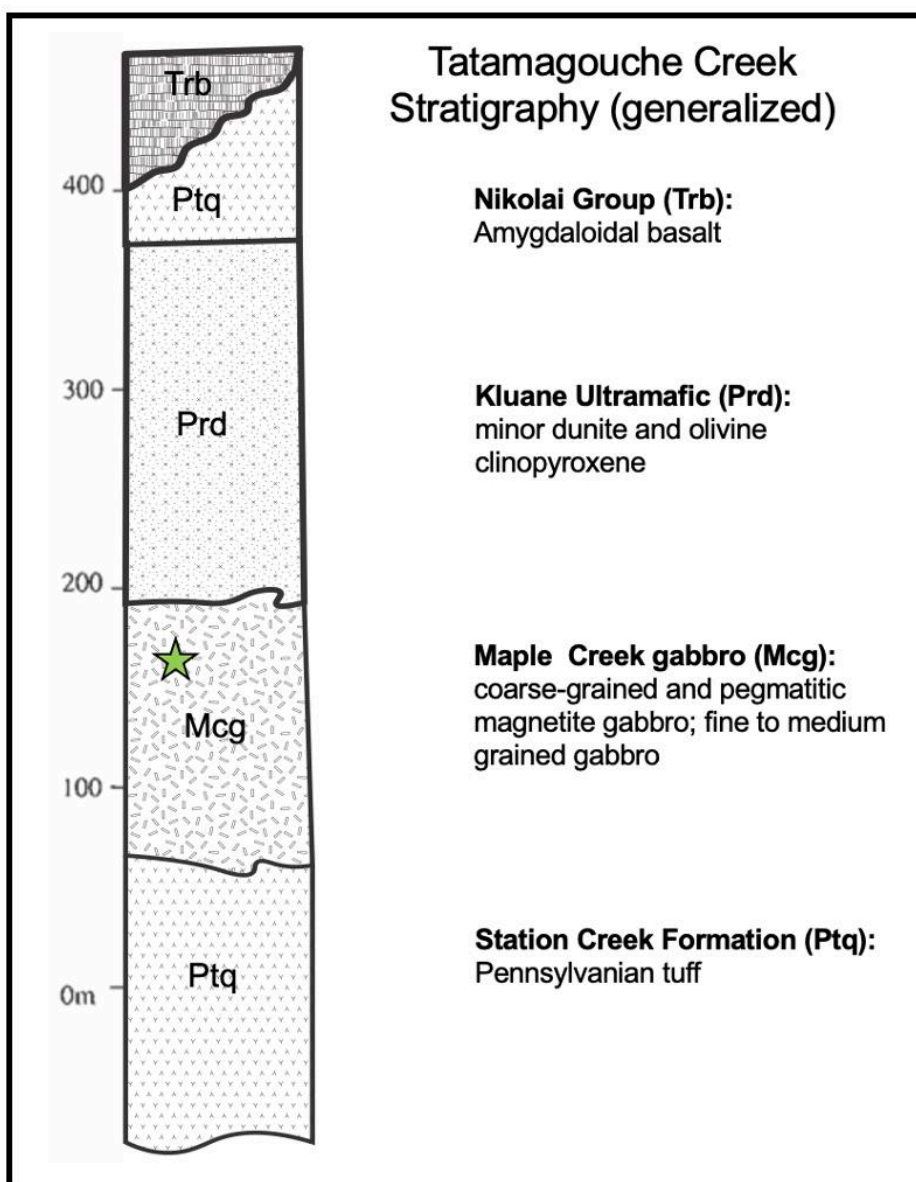


Figure 5: Simplified stratigraphic column for the Tatamagouche Creek area. Modified from Mortensen and Hulbert (1992). The approximate stratigraphic location of the dated sample is indicated by the green star.

Methods:

Samples were prepared and analyzed at the Boise State University Isotope Geology Laboratory using standard laboratory procedures that include crushing, sieving, and annealing samples to isolate and select zircon crystals for TIMS analysis (Macdonald et al., 2018). In addition to traditional separation methods, I used a whole-rock dissolution method (Oliviera et al., 2022) to separate the zircons from the bulk rock. I crushed, sieved, and dissolved a total of six 1–2 kg basalt, gabbro, and ultramafic samples from the Kluane Range (Fig. 4). Six amygdaloidal basalt samples were excluded from consideration because the presence of amygdules—vesicles that have been infilled with other minerals after the basalt cooled—indicating that the basalts are altered (Table 1). I bulk-annealed and used the whole rock dissolution process on four samples from the Maple Creek gabbro and two from the Kluane ultramafic suite. To dissolve the samples and concentrate zircons, I ran them over a water table to separate the crushed material into different densities. I put the sample in ethanol and scooped the crushed rock with a spoon before running the sample over the water table.

Sample Number	UTMN	UTME	Zone	Description	Notes
04-SIS-96-2	579513	6817296	7	Fine-grained, variably amygdaloidal, green to maroon basalt. Amygdules filled locally filled with chlorite/chalcedony. Nikolai formation	Altered
05-SI-56-1	576969	6800729	7	Dark green to brownish/green amygdaloidal pillowed basalt, minor olivine phenocrysts. Nikolai formation	Altered
04-SIS-165-1	587808	6804783	7	Dark green to brown weathered fine to medium-grained gabbro, possible feeder to Nikolai (Maple Creek Gabbro)	Abundant zircon
04-SIS-156-1	593450	6806001	7	Maroon to brick red to olive green amygdaloidal basalt flow with oxidized brecciated flow tops and bottoms; Nikolai formation, fine grained	Altered
04-SIS-185-3	586588	6812129	7	Fine to medium-grained, grey to brownish gabbro intruding Hasen Creek Formation carbonates and siltstone (Maple Creek Gabbro)	no zircon
05-AT-051-1	578748	6797979	7	Amygdaloidal basalt near contact with Chitstone limestone; more than likely Nikolai formation small chance this is Station Creek (Pennsylvanian)	altered
07-RC-024-1	519309	6875858	7	Greenish to maroon, fine-grained basalt, Nikolai formation	altered
04-SIS-085-1	577003	6817880	7	Maroon to brick red to dark green fine-grained, amygdaloidal basalt, Nikolai formation	altered
05-SI-134-1	573743	6815049	7	Olive green amygdaloidal basalt, Nikolai formation	Altered
07-SI-102-1	555279	6836945	7	Medium-grained grey/brown to black pyroxene gabbro intruding Station Creek volcanic rocks; Kluane Mafic-ultramafic suite	no zircon
07-SI-031-1	519857	6875219	7	Fine to medium-grained dark green gabbro, Maple Creek gabbro	no zircon
05-SI-167-3	601199	6795212	7	Medium to fine-grained gabbro sill near lower contact of Nikolai with Hasen Creek Formation; Maple Creek gabbro sill	no zircon
05-SI-150-1	548057	6833198	7	Dark green to light grey, gabbro to pyroxenite, more leucocratic gabbroic portions sampled, Kluane Mafic-ultramafic suite	no zircon

Table 1: List of samples received from the Yukon Geological Survey as potential candidates for the whole rock dissolution process. Of these samples, only one yielded zircon. The amygdaloidal basalt samples showed significant alteration and were excluded from consideration.

Once the bulk rock was crushed and separated, the heaviest split of each sample was annealed at 900° C for 72 hours in a muffle furnace. Annealing the sample at 900° C helps eliminate elemental and isotopic leaching from portions of the zircon crystal that have low to moderate levels of radiation damage (Mattinson, 2005). The annealing process does not affect the U-Pb isotopic system, and the radioisotopic date will not be impacted by annealing the zircons (Mattinson, 2005). After the samples were annealed, they were chemically dissolved. The samples were weighed and placed in 60mm Savilex Beakers. Between 4 to 10 grams of sample was placed in each beaker, and 40 mL of reagent grade acids were added to each beaker. During the first step, I mixed aqua-regia by adding 12M

HCl and 16M HNO₃ on a 3:1 proportion, adding HCl first and then HNO₃. The beakers were capped and placed on a hot plate at 150°C for 24 hours. After the aqua Regia dissolution period, the beakers were removed from the hot plate and cooled for around 3 minutes. After emptying the acid, the samples were rinsed two times with MQH₂O. Once the samples were rinsed, 40 mL of reagent grade 29M hydrofluoric acid was added to the beakers. The beakers were capped loosely to allow fumes to escape. The beakers were placed on a hot plate at 150°C for 24h. After the 29M HF dissolution period, the beakers were removed from the hot plate and cooled for approximately 3 minutes. After emptying the acid, the samples were rinsed two times with MQH₂O. If oxides were still visible at this point, I repeated the aqua Regia dissolution step to dissolve the remaining oxides. After cooling and emptying the acid, the samples were rinsed two times with MQH₂O. Using reagent-grade acids, I added 12M HCl to the beakers. The beakers were placed on the hot plate at 150°C for 2 hours. This step was repeated in two-hour intervals until the sample was completely dissolved.

I dissolved a total of 40 grams of the densest crushed fraction of sample 04-SIS-165-1, which was the only sample that contained zircons. Over 1000 zircons were found in sample 04-SIS-165-1. Fewer than 5 sub-50-micron zircons were found in one of the Kluane-mafic ultramafic suite samples. The TIMS data showed that the zircons from the Kluane- mafic ultramafic sample were Miocene in age, which indicates that they were introduced via laboratory contamination.

Following the whole rock dissolution process, twelve zircons from sample 04-SIS-165-1 were selected and loaded into 300 ml Teflon PFA capsules containing 29M HF, placed in a Parr vessel, and chemically abraded for 12 hours at 190° C, thus removing and

dissolving the most damaged portions of the crystals. All 12 zircons survived the chemical abrasion process (Fig 6).

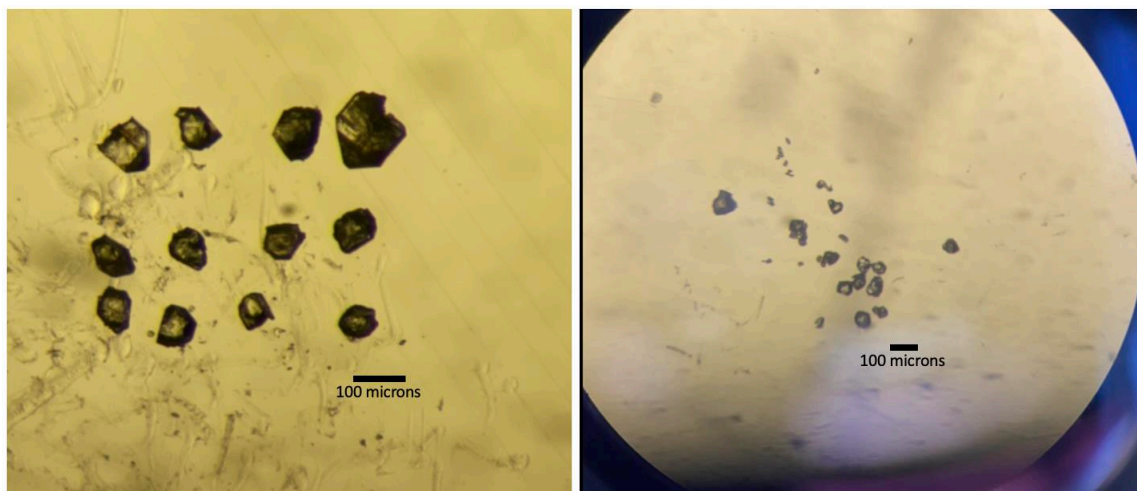


Figure 6: Zircons extracted using the whole rock dissolution method before (left) and after (right) chemical abrasion at 190° C for 12 hours. All 12 grains that were chemically abraded survived the process.

I also chemically abraded 12 zircons from the same sample that were obtained through traditional methods (frantzing, selecting suitable zircons under the microscope, and annealing the zircon after selection). Of the 12 zircons that did not undergo the whole rock dissolution process, only three grains survived chemical abrasion at 190° C. (Fig 7). The three that did survive were severely damaged during chemical abrasion and were deemed unsuitable for CA-IDTIMS analysis.

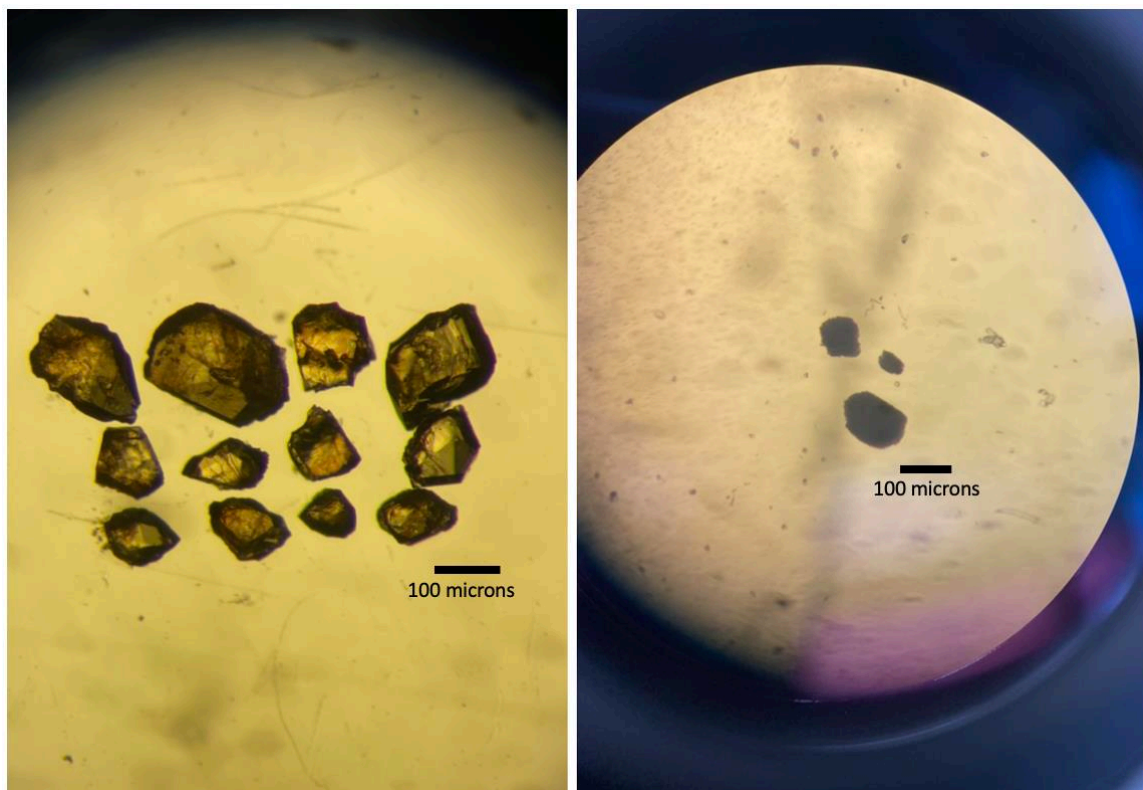


Figure 7: Zircons extracted using traditional methods before (left) and after (right) chemical abrasion at 190 ° C for 12 hours. Only 3 of the 12 grains that were chemically abraded survived the process. None of them were suitable for IDTIMS analysis. This indicates that the whole rock dissolution process eliminated the most metamict and damaged zircons, streamlining the selection process for TIMS analysis.

After chemical abrasion, each zircon was rinsed with 6M HCl and ultrapure H₂O to remove any impurities remaining after chemical abrasion. The 300 ml Teflon PFA microcapsules were fluxed with 6 M HCl to clean them before spiking. Individual zircon grains were loaded into 300 ml Teflon PFA microcapsules and spiked with the EARTHTIME ⁵³⁵ spike. 29 M HF was added to each microcapsule, and the microcapsules were placed in the oven for 48 hours to completely dissolve the samples. 6 M HCL was added after the samples were dried down. They were then placed in the oven overnight at 180° C to convert the fluorides into hydrochloride salt. The uranium and lead were

separated from the zircon matrix by using an HCl based anion-exchange chromatographic procedure (Krogh, 1973) and eluted with 2 μ l of 0.05 N H₃PO₄. The mixed U and Pb material from each zircon were loaded onto single outgassed Re filaments with 5 μ l of a silica-gel/phosphoric acid mixture (Gerstenberger and Haase, 1997).

The filaments were loaded into an Isoprobe-T multicollector thermal ionization mass spectrometer. Pb isotopes were measured on a Daly detector and corrected for $0.16 \pm 0.03\%$ /a.m.u. (1 sigma error) mass fractionation. Uranium isotopes were analyzed in Faraday mode. The known Uranium ratio of the EARTHTIME spike was used to correct for uranium mass fractionation. The EARTHTIME tracer solution was cross calibrated using EARTHTIME gravimetric standards. The Schmitz and Schoene algorithms were used to calculate the CA-TIMS dates and uncertainties. Any common lead present in the analyses was attributed to lab blanks and subtracted from the analysis.

Results:

Of the six samples – four from the Maple Creek gabbro and two from the Kluane Ultramafic suite – that underwent the dissolution process, one yielded zircons (Fig 8). Sample 04-SIS-165-1 is a dark green, medium-grained, with plagioclase crystals approximately 1-2 centimeters long (Fig 8).



Figure 8: Hand sample and zircons from the dated sample 04-SIS-165-1; a sample of the Maple Creek gabbro collected in the Tatamagouche area of the Kluane Range, Yukon. The zircons pictured on the right were collected using the whole rock dissolution method.

U-Th-Pb isotopic data for zircons from Maple Creek Gabbro																				
Sample	Compositional Parameters						Radiogenic Isotope Ratios						Isotopic Ages							
	Th	$^{206}\text{Pb}^*$	mol %	Pb^*	Pb_c	$\frac{^{206}\text{Pb}}{^{204}\text{Pb}}$	$\frac{^{208}\text{Pb}}{^{206}\text{Pb}}$	$\frac{^{207}\text{Pb}}{^{206}\text{Pb}}$	$\frac{^{207}\text{Pb}}{^{204}\text{Pb}}$	$\frac{^{207}\text{Pb}}{^{235}\text{U}}$	$\frac{^{206}\text{Pb}}{^{238}\text{U}}$	corr.	$\frac{^{207}\text{Pb}}{^{206}\text{Pb}}$	$\frac{^{207}\text{Pb}}{^{235}\text{U}}$	$\frac{^{206}\text{Pb}}{^{238}\text{U}}$					
(a)	(b)	(c)	(c)	(c)	(c)	(d)	(e)	(e)	(f)	(e)	(f)	(f)	(g)	(f)	(g)	(f)	(g)			
Sample: 04-SIS-165-1																				
z1	1.1903	3.5331	99.89%	326	0.32	16547	0.378	0.050792	0.066	0.255036	0.128	0.036434	0.064	0.977	230.4	1.5	230.66	0.26	230.69	0.15
z10	0.701	1.0795	99.18%	38	0.74	2196	0.222	0.050714	0.223	0.254910	0.267	0.036472	0.078	0.665	226.79	5.15	230.56	0.55	230.927	0.177
z4	0.938	4.3209	99.53%	72	1.68	3895	0.298	0.050870	0.111	0.255734	0.161	0.036477	0.066	0.840	233.92	2.57	231.22	0.33	230.958	0.149
z2	1.068	10.2084	99.88%	280	1.05	14620	0.339	0.050780	0.068	0.255281	0.128	0.036477	0.064	0.970	229.81	1.57	230.86	0.26	230.959	0.145
z6	0.521	5.2216	99.86%	215	0.61	12859	0.165	0.050822	0.070	0.255541	0.131	0.036484	0.065	0.959	231.73	1.62	231.07	0.27	231.003	0.148
z9	0.864	3.9742	99.86%	229	0.47	12567	0.274	0.050760	0.090	0.256541	0.144	0.036672	0.070	0.870	228.89	2.08	231.88	0.30	232.171	0.160

Table 2: Isotopic data for zircons from Maple Creek Gabbro. (a) z1, z2 etc. are labels for single zircon grains or fragments annealed and chemically abraded after Mattinson (2005); **bold** indicates grains used in final age calculations. (b) Model Th/U ratio iteratively calculated from the radiogenic $^{208}\text{Pb}/^{206}\text{Pb}$ ratio and $^{206}\text{Pb}/^{238}\text{U}$ age. (c) Pb^* and Pb_c represent radiogenic and common Pb, respectively; mol % $^{206}\text{Pb}^*$ with respect to radiogenic, blank, and initial common Pb. (d) Measured ratio corrected for spike and fractionation only. Pb fractionation corrected using mass bias measured in ET535-spiked samples run during the experiment; U fractionation corrected based upon the measured ET535 spike composition during the run. (e) Corrected for fractionation, spike, and common Pb; all common Pb was assumed to be procedural blank: $^{206}\text{Pb}/^{204}\text{Pb} = 18.042 \pm 0.61\%$; $^{207}\text{Pb}/^{204}\text{Pb} = 15.537 \pm 0.52\%$; $^{208}\text{Pb}/^{204}\text{Pb} = 37.686 \pm 0.63\%$ (all uncertainties 1-sigma). (f) Errors are 2-sigma, propagated using the algorithms of Schmitz and Schoene (2007). (g) Calculations are based on the decay constants of Jaffey et al. (1971). $^{206}\text{Pb}/^{238}\text{U}$ and $^{207}\text{Pb}/^{206}\text{Pb}$ ages corrected for initial disequilibrium in $^{230}\text{Th}/^{238}\text{U}$ using $\text{Th}/\text{U} [D] = 0.2 \pm 0.05$.

The zircons from sample 04-SIS-165-1 were uranium-rich and had between 28 to 294 picograms of radiogenic lead, which is considered substantial (Table 2) (Ewing et al., 2003). Analysis of four concordant zircons yielded a weighted mean date of $230.964 \pm$

0.077 Ma (Fig. 9). Two additional zircons were analyzed but were discordant and excluded from the final result (Fig 10).

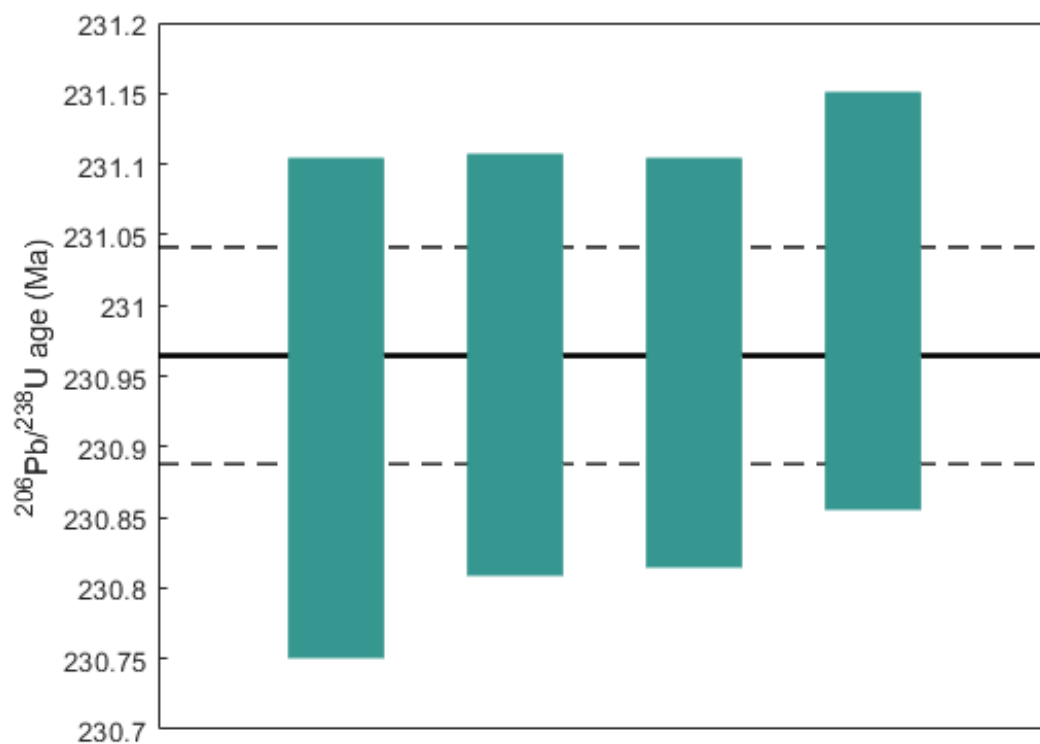


Figure 9: Weighted mean results for sample 04-SIS-165-1. Of the six grains analyzed, two were excluded from the final date calculations. The four concordant zircons from sample 04-SIS-165-1 were used to calculate the mean weighted date and yielded a result of 230.964 with a 2 sigma (find symbol) uncertainty of ± 0.077 Ma.

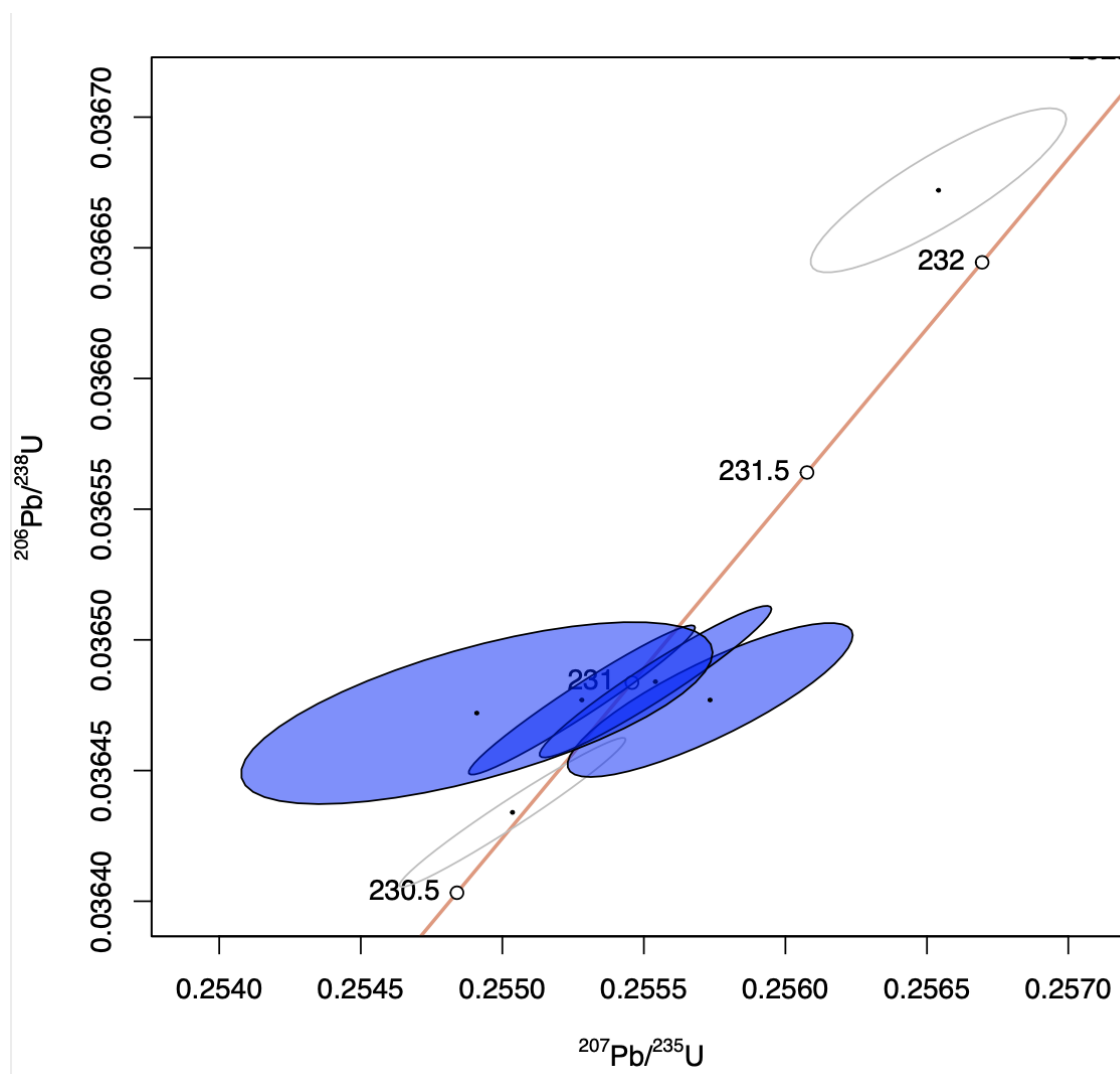


Figure 10: Concordia diagram for sample 04-SIS-165-1. Of the six grains analyzed, two were excluded from the final date calculations. The excluded analyses are shown in light grey, and the analyses used are shown in blue. The oldest analysis was not included because the result was reversely discordant, which may indicate that there was xenocrystic inheritance in that grain. The youngest date was also not included, as the slightly younger date is interpreted to be a result of minor lead loss.

Discussion:

Better age constraints are critical for understanding the relationship between LIP volcanism and Earth system change. In particular, the absence of reliable dates for

Wrangellia volcanism leaves the causes of early Late Triassic environmental evolution poorly constrained (Dal Corso et al., 2020). The date of 230.964 ± 0.077 Ma for the Maple Creek gabbro from this study provides the most accurate and precise timing for Wrangellia magmatism (Fig. 11). The date from this study overlaps within uncertainty with a U-Pb age of 230.91 ± 0.33 Ma from a volcanic ash bed in the Apennine Mountains in southern Italy that stratigraphically overlies the sedimentary record of Carnian environmental change (Furin et al., 2006). The ash bed occurs 3 meters above the marker beds for the top of the CPE interval (Furin et al., 2006). Conodont and palynomorph biostratigraphy indicate that sediment deposition was relatively continuous (Furin et al., 2006), suggesting a limited time interval between the deposition of CPE strata and the ash bed. The ash date is thus considered a minimum age for the processes influencing Carnian environmental change (Gradstein et al., 2020; Dal Corso et al., 2012). In combination, the two dates imply that the younger published dates for Wrangellia are likely less reliable and may reflect problems in analytical approaches. The younger dates may also imply that the most rapid and consequential volcanism and volatile release from the Wrangellia LIP occurred before ~ 230 Ma, which is substantially older than many previous age estimates of Wrangellia emplacement (Greene et al., 2010).

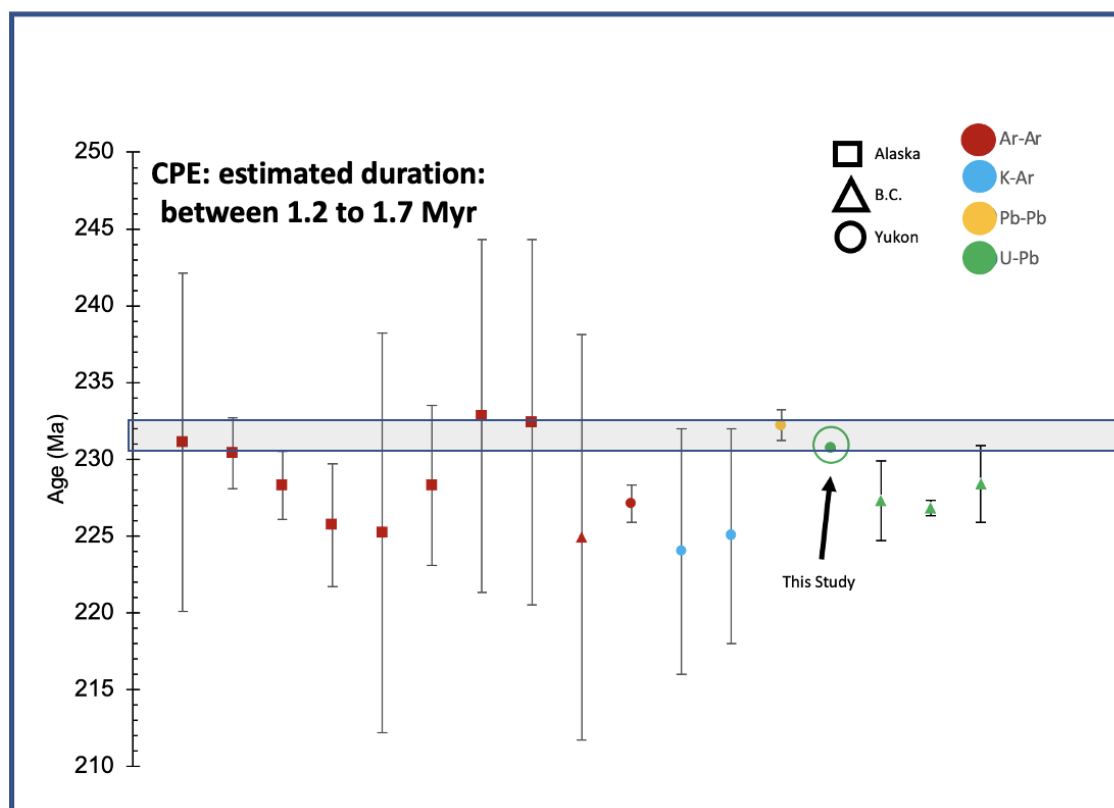


Figure 11: Published radioisotopic dates for the Wrangellia LIP and their corresponding uncertainties, including the date from this study. The dates are separated by method (color) and location (shape) (Schmidt and Rogers, 2007; Greene et al., 2010; Bittenbender et al., 2003; Bittenbender et al., 2007; Lassiter, 1995; Mortensen and Hulbert, 1992; Campbell, 1981; Sluggett, 2003; Parrish and McNicoll, 1992). The grey band denotes the approximate timing and duration of the CPE.

The majority of published radioisotopic dates for Wrangellia were obtained using K-Ar and Ar-Ar dating (Fig. 11) (Greene et al., 2010), and many of the previously published K-Ar and Ar-Ar dates are younger than the date of 230.964 Ma from this study (Fig. 11) (Campbell, 1981; Bittenbender et al., 2003; Bittenbender et al., 2007; Lassiter, 1995; Greene et al., 2010). There are four published radioisotopic dates for Wrangellia exposures in the Yukon, with uncertainties ranging from 1 to 8 Myr (Fig. 9) (Greene et al., 2010; Mortensen and Hulbert, 1992; Campbell, 1981). There is one zircon date (232 ± 1 Ma) (Fig. 9) (Mortensen and Hulbert, 1992), two K-Ar dates ($224 \text{ Ma} \pm 8 \text{ Ma}$ and 225 Ma

± 7 Ma) (Campbell, 1981), and one Ar–Ar (227.5 ± 1.2 Ma) (Fig. 11) (Greene et al., 2010). Though K-Ar and Ar-Ar are commonly used to date mafic rocks, thermal alteration of a system can cause inaccurate results (Kelley, 2002; Schmitz and Kuiper, 2013). Argon degasses during thermal resetting, obscuring the original magmatic signal (Kelley, 2002; Balogh and Simonits, 1998b). Instead of reflecting the date of emplacement, the K-Ar and Ar-Ar dates may reflect the timing of systemic alteration (Kelley, 2002). The Wrangellia flood basalts and their associated intrusive units in the Yukon (the Maple Creek gabbro) underwent burial metamorphism during Late Triassic to Early Jurassic, and a contraction event during the mid-Cretaceous that thermally altered the system (Greene et al., 2010). This alteration likely impacts the reliability of the Ar-Ar and K-Ar dates, making many of the dates erroneously young. Instead of reflecting the emplacement timing for Wrangellia, the younger dates may be the result of Ar-Ar degassing during alteration events after Wrangellia was already emplaced (Greene et al., 2010)

For systems that have undergone thermal alteration, U-Pb zircon geochronology can yield more reliable results (Kelley, 2002; Schmitz et al., 2020). Zircon is a physically robust mineral and is less vulnerable to thermal resetting than Ar-Ar and K-Ar (Schmitz et al., 2020). Currently, there is one published zircon date for the Maple Creek gabbro (Mortensen and Hulbert, 1992). However, the date was calculated using the average $^{207}\text{Pb}/^{206}\text{Pb}$ age of three discordant analyses from multigrain zircon fractions (Mortensen and Hulbert, 1992). Analytical techniques in zircon geochronology have improved substantially since 1992. The implementation of chemical abrasion, using single grain analyses instead of multigrain fractions, and more precise certainties in analytical standards have helped further reduce uncertainties (Mattinson, 2005; Schmitz et al., 2020).

There are three published U-Pb dates for Wrangellia gabbros located near Vancouver Island (Fig.11) (Parrish and McNicoll, 1992; Sluggett, 2003), and the dates range from 226.8 ± 0.5 Ma to 228.4 ± 2.5 Ma. However, the three published U-Pb dates were collected before chemical abrasion was developed (Mattinson, 2005). Chemical abrasion was designed to improve the accuracy and reliability of IDTIMS zircon geochronology by using concentrated hydrofluoric acid to completely remove damaged zones of the zircon crystals before analysis (Mattinson, 2005). As uranium decays, it damages the crystal lattice of the zircon, causing lead atoms to escape the lattice during a process known as 'lead loss' (Chakoumakos et al., 1987; Ewing et al., 2003). Zircons that have not undergone chemical abrasion can provide erroneously young dates because the damaged portions of the zircon that have experienced lead loss have not been completely removed and are still included in the analysis (Mattinson, 2005). The Vancouver Island samples were dated before chemical abrasion was widely adopted, and the dates may be younger than the date from this study because chemical abrasion was not used.

Additionally, the whole rock dissolution process that was used for this study made it easier to select suitable zircon grains for analysis. Because the zircons were uranium rich, the integrity of the crystal lattices were compromised. Though most of the crystals still had metamict zones after undergoing the whole rock dissolution process (Fig. 6), the grains were substantially smaller than the grains obtained using traditional separation methods (Fig. 7), implying that the most damaged portions of the crystals were completely removed during the whole rock dissolution process. This indicates that the whole rock dissolution process also serves as a useful screening method for uranium-rich zircons sourced from mafic rocks.

Summary and Conclusions:

The analyzed date for the Maple Creek Gabbro in this study is the most precise radioisotopic constraint for the timing of the Wrangellia LIP. The overlap within uncertainty between this date and the ash bed date from the southern Apennines, Italy indicates that there is a temporal connection between Wrangellia volcanism and Carnian Earth system change. Younger dates for Wrangellia reflect later-stage volcanism after the main eruptive phase, result from less accurate and precise analytical techniques, or reflect the influence of thermal alteration. More accurate and precise constraints on the timing of Wrangellia emplacement are critical for understanding the long-term connection between large-scale volcanism and Carnian Earth system evolution.

References:

- Balogh, K., and A. Simonits. 1998. “Improvements in Experimental Techniques of Conventional K/Ar and Ar/Ar Geochronological Methods.” *Rapid Communications in Mass Spectrometry: RCM* 12 (22): 1769–70.
- Bernardi, Massimo, Piero Gianolla, Fabio Massimo Petti, Paolo Mietto, and Michael J. Benton. 2018. “Dinosaur Diversification Linked with the Carnian Pluvial Episode.” *Nature Communications* 9 (1): 1499.
- Bittenbender, Peter E., Kirby W. Bean, and Edward G. Gensler. 2003. *Mineral Investigations in the Delta River Mining District, East-Central Alaska, 2001-2002*. U.S. Department of the Interior, Bureau of Land Management, Alaska State Office.
- Bittenbender, P.E., Bean, K.W., Kurtak, J.M., and Deninger, J., Jr., 2007, Mineral assessment of the Delta River Mining District area, east-central Alaska: U.S. Bureau of Land Management-Alaska Technical Report 57, 676 p.,
- Black, Benjamin A., Leif Karlstrom, and Tamsin A. Mather. 2021. “The Life Cycle of Large Igneous Provinces.” *Nature Reviews Earth & Environment* 2 (12): 840–57.
- Bond, David P. G., and Yadong Sun. 2021. “Global Warming and Mass Extinctions Associated with Large Igneous Province Volcanism.” *Large Igneous Provinces*. Wiley. <https://doi.org/10.1002/9781119507444.ch3>.
- Burgess, Seth D., and Samuel A. Bowring. 2015. “High-Precision Geochronology Confirms Voluminous Magmatism Before, During, and after Earth’s Most Severe Extinction.” *Science Advances* 1 (7): e1500470.
- Campbell, Susan Wendy. 1981. “Geology and Genesis of Copper Deposits and Associated Host Rocks in and near the Quill Creek Area, Southwestern Yukon.” University of British Columbia.
- Chakoumakos, Bryan C., Takashi Murakami, Gregory R. Lumpkin, and Rodney C. Ewing. 1987. “Alpha-Decay—Induced Fracturing in Zircon: The Transition from the Crystalline to the Metamict State.” *Science* 236 (4808): 1556–59.
- Csejtey, Béla, Dennis P. Cox, Russell C. Evarts, Gary D. Stricker, and Helen L. Foster. 1982. “The Cenozoic Denali Fault System and the Cretaceous Accretionary Development of Southern Alaska.” *Journal of Geophysical Research*.

<https://doi.org/10.1029/jb087ib05p03741>.

Dal Corso, Jacopo, Alastair Ruffell, and Nereo Preto. 2019. “Carnian (Late Triassic) C-Isotope Excursions, Environmental Changes, and Biotic Turnover: A Global Perturbation of the Earth’s Surface System.” *Journal of the Geological Society*.
<https://doi.org/10.1144/jgs2018-217>.

Dal Corso, Jacopo, Massimo Bernardi, Yadong Sun, Haijun Song, Leyla J. Seyfullah, Nereo Preto, Piero Gianolla, et al. 2020. “Extinction and Dawn of the Modern World in the Carnian (Late Triassic).” *Science Advances* 6 (38).

Erba, Elisabetta. 2006. “The First 150 Million Years History of Calcareous Nannoplankton: Biosphere–geosphere Interactions.” *Palaeogeography, Palaeoclimatology, Palaeoecology* 232 (2): 237–50.

Ewing, Rodney C., Alkiviathes Meldrum, Lumin Wang, William J. Weber, and L. René Corrales. 2003. “Radiation Effects in Zircon.” *Reviews in Mineralogy and Geochemistry* 53 (1): 387–425.

Furin, Stefano, Nereo Preto, Manuel Rigo, Guido Roghi, Piero Gianolla, James L. Crowley, and Samuel A. Bowring. 2006. “High-Precision U-Pb Zircon Age from the Triassic of Italy: Implications for the Triassic Time Scale and the Carnian Origin of Calcareous Nannoplankton and Dinosaurs.” *Geology* 34 (12): 1009–12.

Gerstenberger, H., and G. Haase. 1997. “A Highly Effective Emitter Substance for Mass Spectrometric Pb Isotope Ratio Determinations.” *Chemical Geology*.

Guex, Jean, Sebastien Pilet, Othmar Müntener, Annachiara Bartolini, Jorge Spangenberg, Blair Schoene, Bryan Sell, and Urs Schaltegger. 2016. “Thermal Erosion of Cratonic Lithosphere as a Potential Trigger for Mass-Extinction.” *Scientific Reports* 6 (March): 23168.

Gradstein, Felix M., James G. Ogg, Mark D. Schmitz, and Gabi M. Ogg. 2020. *Geologic Time Scale 2020*. Elsevier.

Greene, Andrew R., James S. Scoates, Dominique Weis, and Steve Israel. 2009. “Geochemistry of Triassic Flood Basalts from the Yukon (Canada) Segment of the Accreted Wrangellia Oceanic Plateau.” *Lithos* 110 (1): 1–19.

Greene, Andrew R., James S. Scoates, Dominique Weis, Erik C. Katvala, Steve Israel, and Graham T. Nixon. 2010. “The Architecture of Oceanic Plateaus Revealed by the Volcanic Stratigraphy of the Accreted Wrangellia Oceanic Plateau.” *Geosphere* 6 (1): 47–73.

- Hillihouse, J. W. (1977). Paleomagnetism of the Triassic Nikolai Greenstone, McCarthy Quadrangle, Alaska. *Canadian Journal of Earth Sciences* 14, 2578-3 592. Hillhouse, J. W. & Coe, R. S. (1994). Paleomagnetic data from Alaska. In: Plaficer, G. & Berg, H. C. (eds.) *The Geology of Alaska*. Geological Society of America
- Hulbert, L. J. 1997a. "Geology and Metallogeny of the Kluane Mafic-Ultramafic Belt, Yukon Territory, Canada: Eastern Wrangellia - a New Ni-Cu-PGE Metallogenic Terrane." Geological Survey of Canada. <https://doi.org/10.4095/208992>.
- Israel, Tizzard, Major, and Emond. n.d. "Bedrock Geology of the Duke River Area, Parts of NTS 115G/2, 3, 4, 6 and 7, Southwestern Yukon." *Andean Geology*.
- Jones, David L., N. J. Silberling, and John Hillhouse. 1977. "Wrangellia—A Displaced Terrane in Northwestern North America." *Canadian Journal of Earth Sciences* 14 (11): 2565–77.
- Kelley. n.d. "K-Ar and Ar-Ar Dating." *Reviews in Mineralogy and Geochemistry*. <https://www.geo.arizona.edu/~reiners/geos474-574/Kelley2002.pdf>.
- Konstantinov, Konstantin M., Mikhail L. Bazhenov, Anna M. Fetisova, and Mikhail D. Khutorskoy. 2014. "Paleomagnetism of Trap Intrusions, East Siberia: Implications to Flood Basalt Emplacement and the Permo–Triassic Crisis of Biosphere." *Earth and Planetary Science Letters* 394 (May): 242–53.
- Krogh, T. E. 1973. "A Low-Contamination Method for Hydrothermal Decomposition of Zircon and Extraction of U and Pb for Isotopic Age Determinations." *Geochimica et Cosmochimica Acta* 37 (3): 485–94.
- Lassiter, John Channing. 1995. "Geochemical Investigations of Plume-Related Lavas: Constraints on the Structure of Mantle Plumes and the Nature of Plume/lithosphere Interactions." Edited by Donald J. DePaolo. Ann Arbor, United States: University of California, Berkeley.
- Lu, Jing, Peixin Zhang, Jacopo Dal Corso, Minfang Yang, Paul B. Wignall, Sarah E. Greene, Longyi Shao, Dan Lyu, and Jason Hilton. 2021. "Volcanically Driven Lacustrine Ecosystem Changes during the Carnian Pluvial Episode (Late Triassic)." *Proceedings of the National Academy of Sciences of the United States of America* 118 (40). <https://doi.org/10.1073/pnas.2109895118>.
- Macdonald, Francis A., Mark D. Schmitz, Justin V. Strauss, Galen P. Halverson, Timothy M. Gibson, Athena Eyster, Grant Cox, Peter Mamrol, and James L. Crowley. 2018. "Cryogenian of Yukon." *Precambrian Research* 319 (December): 114–43.
- Martindale, Rowan C., William J. Foster, and Felicitás Velledits. 2019. "The Survival, Recovery, and Diversification of Metazoan Reef Ecosystems Following the End-Permian

Mass Extinction Event.” *Palaeogeography, Palaeoclimatology, Palaeoecology* 513 (January): 100–115.

Mattinson, James M. 2005. “Zircon U–Pb Chemical Abrasion (‘CA-TIMS’) Method: Combined Annealing and Multi-Step Partial Dissolution Analysis for Improved Precision and Accuracy of Zircon Ages.” *Chemical Geology*.
<https://doi.org/10.1016/j.chemgeo.2005.03.011>.

Mortensen, J. K., and L. J. Hulbert. 1992. “A U-Pb Zircon Age for a Maple Creek Gabbro Sill, Tatamagouche Creek Area, Southwestern Yukon Territory.” *Bulletin Geological Survey of Canada*.

Oliveira, A. L., Schmitz, C. J. Wall, and M. H. B. M. Hollanda. 2022. “A Bulk Annealing and Dissolution-Based Zircon Concentration Method for Mafic Rocks.” *Chemical Geology* 597 (May): 120817.

Panuska, B. C. n.d. “An Overlooked, World Class Triassic Flood Basalt Event.” *Geological Society of America Bulletin*.

Parrish, and McNicoll. n.d. “U-Pb Age Determinations from the Southern Vancouver Island Area, British Columbia.” *Radiogenic Age and Isotopic Studies: Report*.

Richards, M. A., D. L. Jones, R. A. Duncan, and D. J. Depaolo. 1991. “A Mantle Plume Initiation Model for the Wrangellia Flood Basalt and Other Oceanic Plateaus.” *Science* 254 (5029): 263–67.

Schaller, Morgan F., James D. Wright, and Dennis V. Kent. 2015. “A 30 Myr Record of Late Triassic Atmospheric pCO₂ Variation Reflects a Fundamental Control of the Carbon Cycle by Changes in Continental Weathering.” *GSA Bulletin* 127 (5-6): 661–71.

Schmidt, J. M., and R. K. Rogers. 2007. “Metallogeny of the Nikolai Large Igneous Province (LIP) in Southern Alaska and Its Influence on the Mineral Potential of the Talkeetna Mountains.”

Schmitz, Mark D., and Klaudia F. Kuiper. 2013. “High-Precision Geochronology.” *Elements* 9 (1): 25–30.

Schmitz, Mark D., and Blair Schoene. 2007. “Derivation of Isotope Ratios, Errors, and Error Correlations for U-Pb Geochronology using ²⁰⁵Pb-²³⁵U-(²³³U)-Spiked Isotope Dilution Thermal Ionization Mass Spectrometric Data.” *Geochemistry, Geophysics, Geosystems* 8 (8).

Schmitz, B. S. Singer, and A. D. Rooney. 2020. “Chapter 6 - Radioisotope Geochronology.” In *Geologic Time Scale 2020*, edited by Felix M. Gradstein, James G. Ogg, Mark D. Schmitz, and Gabi M. Ogg, 193–209. Elsevier.

Schoene, Blair, Jean Guex, Annachiara Bartolini, Urs Schaltegger, and Terrence J. Blackburn. 2010. "Correlating the End-Triassic Mass Extinction and Flood Basalt Volcanism at the 100 Ka Level." *Geology* 38 (5): 387–90.

Schoene, Blair, Kyle M. Samperton, Michael P. Eddy, Gerta Keller, Thierry Adatte, Samuel A. Bowring, Syed F. R. Khadri, and Brian Gertsch. 2015. "U-Pb Geochronology of the Deccan Traps and Relation to the End-Cretaceous Mass Extinction." *Science* 347 (6218): 182–84.

Sluggett. n.d. "Uranium-Lead Age and Geochemical Constraints on Paleozoic and Early Mesozoic Magmatism in Wrangellia Terrane, Saltspring Island, British Columbia [B]" *Canada, University of British Columbia*.

Wignall, P. B. 2001. "Large Igneous Provinces and Mass Extinctions." *Earth-Science Reviews* 53 (1): 1–33.

Yole, R. W. & Irving, E. (1980). Displacement of Vancouver Island, paleomagnetic evidence from the Karmutsen Formation. *Canadian Journal of Earth Sciences* 17, 1210-1228.